

## MINI REVIEW

[View Article Online](#)  
View Journal | View Issue



Cite this: *Ind. Chem. Mater.*, 2024, 2, 556

# Coordination bond cleavage of metal–organic frameworks and application to flame-retardant polymeric materials

Kunpeng Song, Ye-Tang Pan, \* Jiyu He and Rongjie Yang

The physicochemical properties of metal–organic frameworks (MOFs) are closely dependent on the topology, pore characteristics, and chemical composition, which can be tuned through targeted design. Relative to direct synthesis, the post-synthesis methods of MOFs, including ion exchange, ligand replacement as well as destruction, provide a significant increase in their application range and potential. A method based on the coordination bond cleavage of MOFs has been proved to be very effective in modulating the structure and was evaluated for its application in the flame retardant field. Herein, the construction of peculiar MOF structures is categorized based on flame-retardant features through the cleavage of coordination bonds at the molecular level, and the corresponding MOFs exhibit superior flame-retardant and smoke-suppressing properties. Different approaches are highlighted to achieve coordination bond breaking to modulate MOFs properties, involving chemical composition, topology, and pore structure. This review systematically summarizes and generalizes the direct construction of high-efficiency MOF-based flame retardants based on the structure–activity relationship and their further functionalization through coordination bond cleavage, as well as the associated challenges and prospects. It is also hoped that this work will quickly guide researchers through the field and inspire their next studies.

**Keywords:** Metal–organic frameworks; Fire retardancy; Molecular cleavage; Coordination bond; Flame retardant mechanism.

Received 16th October 2023,  
Accepted 23rd November 2023

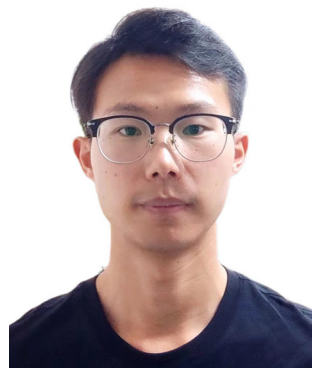
DOI: 10.1039/d3im00110e

rsc.li/icm

## 1 Introduction

Metal–organic frameworks (MOFs) composed of metal nodes and organic linkers are a class of widely studied reticular inorganic–organic complexes.<sup>1–4</sup> The versatility of these star

National Engineering Research Center of Flame Retardant Materials, School of Materials Science & Engineering, Beijing Institute of Technology, Beijing 100081, P.R. China. E-mail: [pyt@bit.edu.cn](mailto:pyt@bit.edu.cn)



Kunpeng Song

*Mr. Kunpeng Song is currently a Ph.D. candidate at the School of Materials Science & Engineering, Beijing Institute of Technology. He has been working in Professor Rongjie Yang's group since 2021. His interests mainly involve the design and preparation of functional MOF-based flame retardants.*



Ye-Tang Pan

*Prof. Ye-Tang Pan received his Ph.D. degree from Polytechnic University of Madrid in 2018, supervised by Prof. De-Yi Wang. Then, he joined the National Engineering Research Center of Flame Retardant Materials, Beijing Institute of Technology, as an Assistant Professor and was promoted to an Associate Professor in 2022. His research interests comprise the controllable preparation of nanomaterials, the design and synthesis of new flame retardants, and multifunctional flame-retardant polymer nanocomposites.*



materials also facilitates the improvement of the flame retardancy of industrial polymeric materials.<sup>5</sup> Since the introduction of MOFs-based flame retardants (FRs) in 2017,<sup>6</sup> the subsequent research studies presented a tremendous rise in this field.<sup>7</sup> The flame-retardant properties exhibited by MOFs depend on their composition, topology, and pore structure. The metal portion mainly includes Zn, Co, Fe, or Zr. Such transition metals enable the catalysis of char formation, while the ligand portion (especially N-containing series) provides the flame-retardant element, and the organic feature benefits the compatibility with the matrix. To date, typical MOFs, namely ZIFs, MILs, and UiOs, are the most popular objects of study.<sup>8–11</sup>

Notably, MOFs applied alone do not confer high limiting oxygen index (LOI) values and UL-94 vertical combustion ratings to polymer composites. This is owing to the single flame-retardant element, low percentage of flame-retardant elements, flammability of ligands, and microporous-dominated pore structure that is difficult to be fully utilized. Although most MOFs are compatible with the matrix, the high surface energy makes it difficult to avoid agglomeration, which undoubtedly makes processing more challenging. Therefore, the design and development of MOF-based flame retardants are particularly essential.<sup>8</sup>

Moreover, post-synthesis (top-down) approaches have received increasing research attention. This strategy allows for flexible modulations of the structure of the as-synthesized MOFs.<sup>12</sup> Weakening of the coordination bond energy of the metal-linker facilitates the post-synthesis of MOFs.<sup>13</sup> The properties of MOF precursors are partially inherited, while more diverse properties are bestowed in the chemical/thermal treatment process. Herein, we focus on post-synthesis approaches involving selective coordination bond cleavage to create new structures and tailor composites.

The post-treatment of MOFs can be briefly categorized into the following three distinct approaches: 1) incorporation of foreign metal ions or ligands into the original structure by

means of exchange reactions; 2) integration of linkers on unstable/empty sites of the structure by solvent-assisted methods; 3) partial disruption into a new structure.<sup>14,15</sup>

Herein, for the first time, we critically evaluate the post-synthesis methods involving coordination bond cleavage in the flame-retardant field in order to tailor composites and structures with or without disrupting the reticulation chemistry of the parent matrix of MOFs. We conclude with a critical outlook on the applications, challenges, and future prospects of this emerging and evolving field.

## 2 Strategies for the cleavage of MOFs into FRs

Template derivatization of MOFs is considered to be an effective strategy for the preparation of structurally functionalized materials. However, the typically generated metal-carbon compounds dramatically depend on uncontrollable heat treatments with high-energy consumption.<sup>16,17</sup> Costly organic ligands are cracked into gases and spilled at high temperatures, accompanied by intrinsic structural contraction, and leaving carbon structures with scarce functional components. Therefore, the pseudomorphic cleavage of MOFs based on the ion/ligand exchange strategy is more facile, gentle, and controllable, and is also increasingly investigated in many fields.<sup>18</sup> MOFs possess inherent flame-retardant potentials, *i.e.*, large specific surface area, well-defined pore structure, and tunable physicochemical properties, and the above strategies also provide feasible insights into the flame-retardant functionalization of MOFs. Recent published papers, which focus on the cleavage of MOFs into FRs, are summarized in Table 1.

### 2.1 Salt hydrolysis

Acid-base strength mismatch leads to the pH value being far from 7 for the corresponding salt during hydrolysis. Alkaline



Jiyu He

*Prof. Jiyu He received his B.S. (1992), M.S. (1997), and Ph.D. (2004) degrees from Beijing Institute of Technology. Currently, he is a Full-time Professor at the School of Materials Science & Engineering, Beijing Institute of Technology. His research interests focus on ablative and flame-retardant materials, propellant materials, and functional polymer materials.*



Rongjie Yang

*Prof. Rongjie Yang received his B.S. (1983) and M.S. (1986) degrees at Beijing Institute of Technology and his Ph.D. degree (1989) from Institute of Chemistry, Chinese Academy of Sciences. Currently, he is a Full-time Professor at Beijing Institute of Technology and the director of the National Engineering Research Center of Flame Retardant Materials. His research interests include flame-retardant polymer materials, high temperature and ablation resistant polymer materials, and special functional polymer materials.*



**Table 1** Summary of the flame-retardant properties of the cleavage of MOFs into FRs

Polymer systems	Type of FRs	Loading (wt%)	Main flame-retardant results	Ref.
Epoxydihedraz C/DDDS	DOPO-loaded pATH	10.0	27.1% of LOI; UL-94 V-0 rating (0.6 mm thickness); 59.3%, 45.8%, and 30.0% reduction in pHRR, THR, and TSP (heat flux of 50 kW m <sup>-2</sup> ; 4 mm thickness)	18
Thermoplastic polyurethane	NiCo-LDH/MoS <sub>2</sub>	2.0	30.9% and 55.7% reduction in pHRR and the peak smoke production rate (PSPR) (heat flux of 50 kW m <sup>-2</sup> ; 3 mm thickness)	28
Epoxydihedraz C/DDDS	rGO@LDH	2.0	65.9%, 16.7%, and 30.0% reduction in pHRR, THR, and TSP (heat flux of 50 kW m <sup>-2</sup> ; 4 mm thickness)	29
Unsaturated polyester resin	GO@LDHs	2.0	35.5%, 27.4%, and 27.7% decrease in pHRR, THR, and TSP (heat flux of 35 kW m <sup>-2</sup> ; 3 mm thickness)	30
Unsaturated polyester resin	CNTs@LDHs	2.0	30.5%, 24.6%, and 22.7% decrease in pHRR, THR, and TSP (heat flux of 35 kW m <sup>-2</sup> ; 3 mm thickness)	30
E-44/DDDS	MgAl@NiCo	2.5	UL-94 V-0 rating (3.2 mm thickness); 66.7%, 38.7%, and 25.0% reduction in pHRR, THR, and TSP (heat flux of 50 kW m <sup>-2</sup> ; 3 mm thickness)	31
Wood fiber/poly(lactic acid)	Ni-PO/APP	5.0/5.0	25.6%, 22.0%, and 43.1% reduction in pHRR, THR, and TSP (heat flux of 35 kW m <sup>-2</sup> ; 3 mm thickness)	35
E-51/DDM	PA-ZIF67@ZIF8	5.0	29.3% of LOI; UL-94 V-0 rating (3 mm thickness); 42.2%, 33.0%, and 41.5% reduction in pHRR, THR, and PCOPR (heat flux of 35 kW m <sup>-2</sup> ; 3 mm thickness)	40
E-44/DDDS	ZNs-B/CP	2.0	28.4% of LOI; 43.1%, 11.9%, and 17.9% reduction in pHRR, THR, and TSP (heat flux of 50 kW m <sup>-2</sup> ; 3 mm thickness)	39
E-44/DDDS	MPOFs	2.0	26.5% of LOI; 35.7%, 10.0%, and 26.1% reduction in pHRR, THR, and TSP (heat flux of 50 kW m <sup>-2</sup> ; 3 mm thickness)	41
Poly(lactic acid)	C <sub>2</sub> N (CNO)	2.0	Promote self-extinguish of the PLA matrix (heat flux of 35 kW m <sup>-2</sup> ; 3 mm thickness)	46
E-44/DDDS	m-CBC@LDH	2.0	29.1% of LOI; 38.5%, 19.6%, and 29.0% reduction in pHRR, THR, and TSP (heat flux of 50 kW m <sup>-2</sup> ; 3 mm thickness)	27
E-44/DDDS	CPPHS	2.0	27.6% of LOI; 40.1% and 38.8% reduction in pHRR and TSP (heat flux of 50 kW m <sup>-2</sup> ; 3 mm thickness)	50

imidazolate ligands in ZIFs are prone to protonation by the H<sup>+</sup> released from the salt-contained aqueous solution, followed by the collapse of the frameworks.<sup>19</sup> We pioneered the correlational research as early as 2017 that honeycomb-like aluminum hydroxide flakes were fabricated by using aluminum nitrate (aq.) to attack ZIF-8 aggregates, as illustrated by the cartoon diagram in Fig. 1a.<sup>18</sup> The removal of rhombic dodecahedra with the residual of the outer coated layer resulted in mesoporous Al(OH)<sub>3</sub>, which could be further loaded with a phosphorus-based flame retardant to improve the fire safety of epoxy resin (EP), superior to the commercial counterparts (Fig. 1b–e).

Over the last decade, the growth of layered double hydroxides (LDHs) from chemically treated MOF precursors is another emerging trend to realize the transformation from one functional material to another. (i) Metal sites in MOFs, as nuclear sites for LDHs, have favorable dispersion and avoid self-stacking; (ii) the larger surface area facilitates the exposure of more active sites; (iii) the well-preserved porous structure creates channels for molecular movement and increases accessibility of LDHs; (iv) recovery of organic ligands detached from the framework by OH<sup>-</sup> substitution is valuable and economical for large-scale industrial production.<sup>15,20</sup> Fortunately, LDHs are just right fillers to improve the fire safety of synthetic polymers. In detail, the decomposition of LDHs produces refractory oxides on the surface of the composite, while releasing water vapor and carbon dioxide. The heat absorption and dilution associated with this process inhibit the thermal feedback during combustion.<sup>21</sup> However, traditional LDHs preparation

methods (such as hydrothermal, ion exchange, and coprecipitation) usually have poor control over the morphology, particle size, and specific surface area, which greatly limits their application. Inspired by the ion-exchange method, the MOFs as sacrificial templates for the construction of LDHs with controlled morphology (*e.g.*, two-dimensional lamellar structures or three-dimensional hollow structures) are considered a promising approach to the above challenges.<sup>8</sup> The most extensively studied prototype is NiCo-LDH evolved from ZIF-67 with the help of nickel nitrate, the hydrolysis of which provides H<sup>+</sup> to separate Co and imidazole, followed by the emergence of an alkaline environment liable to the coprecipitation of Ni and oxidized Co.<sup>22</sup> ZIF-67-derived LDHs have the advantages of higher specific surface area, highly exposed active sites, and excellent catalytic char-forming capability, but the small layer spacing and high surface energy make it difficult to disperse well in the polymer.<sup>23</sup> Therefore, it is also rarely applied to flame-retardant polymers alone, but is further modified. This will be elaborated later. Zammarano *et al.* also elaborated that the unique flame retardancy possessed by LDHs-modified epoxy nanocomposites is mainly due to its nanoscale dispersion level and intrinsic properties.<sup>21</sup> In order to meet the flame retardant requirements, LDHs are usually used in combination with other flame retardants to obtain a synergistic flame retardant effect.<sup>24</sup> Well-exfoliated LDHs in the polymer matrix could exert a physical barrier effect to elongate the escape path for the combustible volatiles, and endothermic action happens during degradation to cool the flame.<sup>25,26</sup> However, ZIF-derived LDHs possess a lower aspect





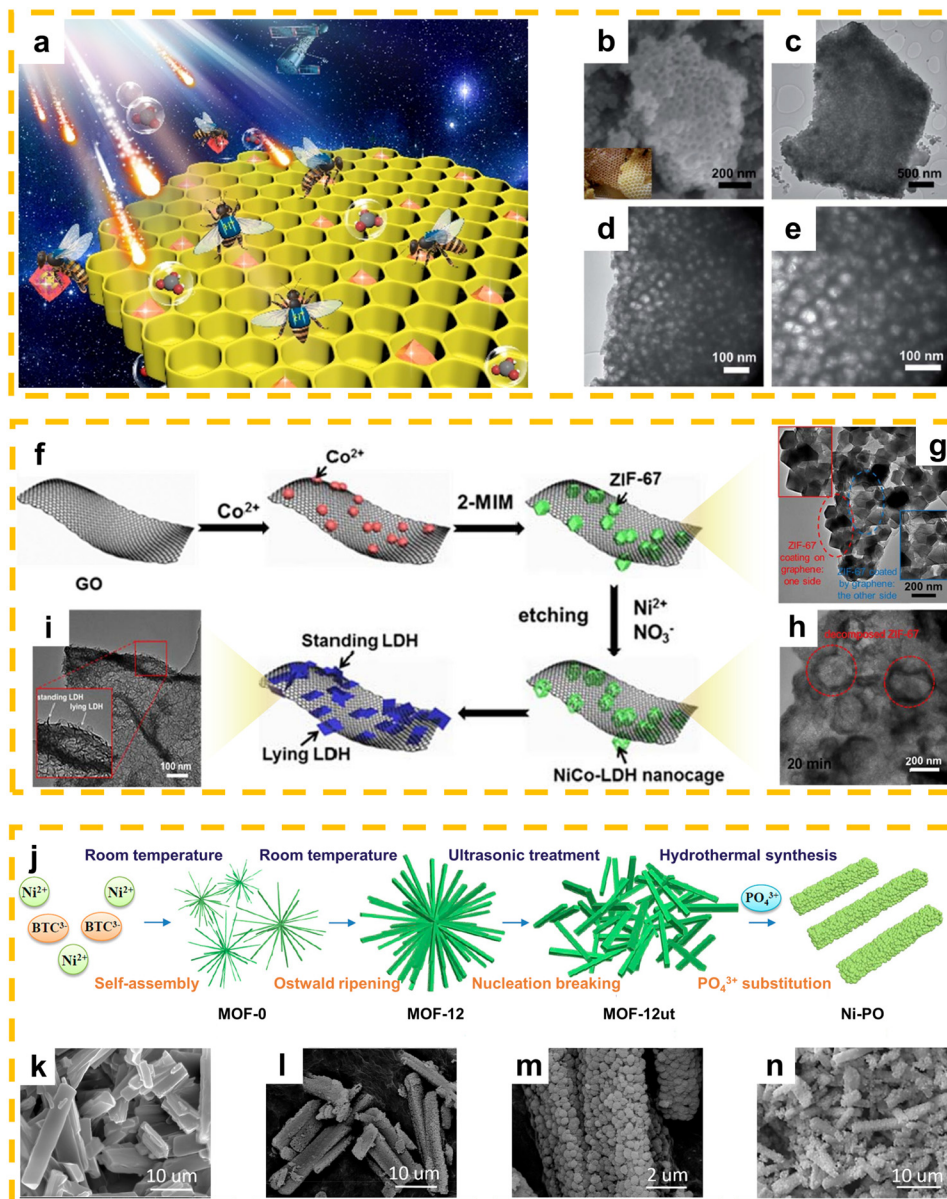


**Fig. 1** (a) An illustration of mesoporous  $\text{Al}(\text{OH})_3$  obtained by salt hydrolyzing treatment to  $\text{ZIF-8}$ ; (b) SEM image (inset: digital photograph of a honeycomb); (c) TEM image and (d and e) enlarged TEM images of mesoporous  $\text{Al}(\text{OH})_3$ . Reproduced from ref. 18 with permission from the Royal Society of Chemistry, copyright 2017. (f) A schematic illustration of the preparation of  $\text{rGO@LDH}$ ; (g–i) the corresponding TEM image of  $\text{rGO@ZIF-67}$ ,  $\text{rGO@LDH}$  nanocage, and  $\text{rGO@LDH}$ . Reproduced from ref. 29 with permission from Elsevier, copyright 2017. (j) A schematic diagram of the morphological evolution from  $\text{Ni-MOF}$  to  $\text{Ni-PO}$ ; the SEM morphology of (k)  $\text{Ni-MOF}$ , (l and m)  $\text{Ni-PO}$ , and (n) re-synthesized  $\text{Ni-PO}$ . Reproduced from ref. 35 with permission from the American Chemical Society, copyright 2019.

ratio than directly synthesized ones, impairing their effect as obstacles for the fuels.<sup>27</sup> Two-dimensional nanomaterials, such as graphene and boron nitride, can be loaded with other nanomaterials to allow them to be well dispersed. The main mechanism of 2D nanomaterials as FRs is their excellent physical barrier effect. However, some problems faced by 2D nanomaterials, such as the interlayer van der Waals forces, make them prone to forming agglomerates, and smooth and inert surfaces are not conducive to their dispersion in the matrix, which seriously affect the comprehensive properties of the composite materials.<sup>28</sup> LDHs

systems can be used to improve the compatibility of two-dimensional materials with a polymer matrix due to their rough surface and abundance of oxygen-containing groups. Generally,  $\text{ZIF-67}$  is firstly anchored on 2D nanomaterials and then transferred into  $\text{NiCo-LDH}$ .<sup>8</sup> As early as 2017, our group proposed a ‘3D fabrication method’ to construct sandwich-structured graphene/layered double hydroxide hybrids ( $\text{rGO@LDH}$ ) using graphene oxide-loaded  $\text{ZIF-67}$  composites as precursors (Fig. 1f–i).<sup>29</sup> The peak of the heat release rate (pHRR), total heat release (THR), and total smoke production (TSP) of the epoxy composites treated with only 2.0 wt%

rGO@LDH were reduced by 65.9%, 16.7%, and 30.0%, respectively, compared to pure epoxy. Hou *et al.* also concluded that Co–Ni LDHs loaded on GO have superior advantages over carbon nanotubes (CNTs) in suppressing the heat and smoke release of composites.<sup>30</sup>

Furthermore, our group reported a novel dual layered double hydroxide hybrid, MgAl-LDH@NiCo-LDH (MgAl@NiCo), in which NiCo-LDH nanosheets derived from ZIF-67 are uniformly anchored on MgAl-LDH.<sup>31</sup> This “3D manufacturing method” can alleviate the disadvantages of agglomeration and low flame retardant efficiency of MgAl-LDH. By adding only 2.5 wt% MgAl@NiCo, the pHRR of the prepared epoxy composite decreased by 66.7% compared to that of pure EP, and passed the V-0 rating in the UL-94 test. The nickel-based and cobalt-based nanocatalysts uniformly dispersed between the MgAl-LDH and polymer interfaces catalyze the surrounding region to form a strong char layer, reducing the transfer of heat and combustible volatiles.<sup>32</sup>

## 2.2 Ligand substitution

The flame-retardant effect of MOFs used alone is not outstanding relative to the reported novel flame retardants.<sup>33,34</sup> One of the main reasons is that a large number of flammable ligands contained in their structures do not contribute to the flame-retardant performance. The flame-retardant functional substitution of the original ligands through the ligand replacement strategy provides good insight for improving the flame-retardant capability of MOFs. Since the chemical stability of MOFs is relatively shaky, the original organic ligand can be replaced by a steadier one. We once prepared regular micro-sized metal phosphate derived from MOFs through substitution of organic linkers with phosphoric ions (Fig. 1j).<sup>35</sup> In detail, Ni-MOF consisting of benzene-1,3,5-tricarboxylic acid as a ligand reacted with Na<sub>3</sub>PO<sub>4</sub> under hydrothermal condition. Then, the hierarchically mesoporous nickel phosphate (Ni-PO) was obtained through substitution of organic linkers with the phosphoric ions. The rod-like Ni-MOF after topological transformation retained the overall profile, but the secondary building units turned into sub-micron particles, as shown in Fig. 1k–m. Notably, the recovery of the Ni-MOF template from the waste solvent after the hydrothermal synthesis of Ni-PO was concluded by us as a sustainable and cost-effective strategy (Fig. 1n). The cone test showed a 43% decrease in TSP when 5.0 wt% ammonium polyphosphate was substituted by Ni-PO in the intumescent flame-retardant wood fiber/poly(lactic acid) system.

## 2.3 Acid etching and alkali etching

One of the primary reasons for the instability of most MOF crystals is the coordination of soft metal cations (Cu<sup>2+</sup>, Ni<sup>2+</sup>, Zn<sup>2+</sup>, Co<sup>2+</sup>, *etc.*) with hard carboxylic acid ligands to form soft and hard compounds, which is inconsistent with the principle of hard and soft acids and bases (HSAB).<sup>36</sup> A number of stabilized MOFs have been successfully

constructed based on high-valent metal ions and carboxylic acid-based ligands under the guidance of HSAB theory. Typical examples involve the MIL, UiO, MOF, USTC, PCN and DUT series.<sup>37,38</sup> These MOFs generally present higher stability in neutral and acidic aqueous solutions.

However, for ZIFs composed of basic ligands, acidic compounds can cleave their covalent bonds more easily, caused by the ionized H<sup>+</sup> protonated ligands. Typically, strong acids can easily protonate imidazole ligands, while weak acids require drastic reaction conditions.<sup>39</sup> Phytic acid is abundant in phosphorus and has adjustable acidity, being an ideal etchant for ZIFs to improve their flame-retardant properties.<sup>40</sup> Our group prepared hollow nanocages carrying ZIF-67 nanodots (ZNs-B/CP) by a step-by-step etching strategy using ZIF-67 as a template as well as phytic acid and boric acid as etching agents, respectively (Fig. 2a–c).<sup>39</sup> This is also the first time that ZIFs nanodots have been explored in the flame retardant field. At only 2.0 wt% loading, the pHRR, THR, and TSP of the epoxy composites can be reduced by 43.1%, 11.9%, and 17.9%, respectively, relative to pure epoxy resins. Impressively, simply switching the order of the two etchants in the same synthesis procedure did not yield this peculiar structure with the accompanying problem of agglomeration. We suggest that phytic acid simultaneously forms cobalt phytate on its outer surface during etching of ZIF-67, which has good chemical stability and protects the integrity of the framework. Furthermore, the released cobalt ions are reassembled on the framework surface to form ZIFs nanodots.

Inspired by this, octacarboxyl POSS (OCP) ingeniously served as both etchant and complexing agent for ZIF-67 to obtain novel metal POSS–organic frameworks (MPOFs) with high specific surface area (393.4 m<sup>2</sup> g<sup>−1</sup>).<sup>41</sup> In addition, a unique “size effect” was noticed due to the difference in the pore diameter of ZIF-67 (1.1 nm) and the size of the OCP (>2.0 nm) (Fig. 2d). That is, the flexible organic groups are accessible, but the rigid inorganic cage is blocked from the outside (Fig. 2e–g). The cone test indicated the 35.7% and 26.1% decrease in pHRR and TSP, respectively, when 2.0 wt% of filler was introduced into the epoxy system.

Alternatively, for water-stabilized MOFs, *e.g.*, MIL-100(Fe) or UiO-66(Zr), selective acid etching can be performed depending on their window size.<sup>38</sup> The process is controlled by the selective diffusion of the acid molecules through the size of the MOFs window. The universality of the strategy was confirmed by selecting inorganic acids, such as phosphoric acid, sulfuric acid, and phosphotungstic acid.<sup>42</sup> However, hydrochloric acid, due to its small molecular dimension, diffuses indiscriminately in the window of MOFs, thus losing size selectivity and leading to structure collapse. This strategy provides a new inspiration for the design of high efficiency and functional flame-retardant materials based on hierarchical MOFs.

As a reverse course of the crystal growth of MOFs, their decomposition can be recognized as the fracture and recombination of coordination bonds, forming amorphous phases or soluble fragments.<sup>43</sup> The dissociation process of



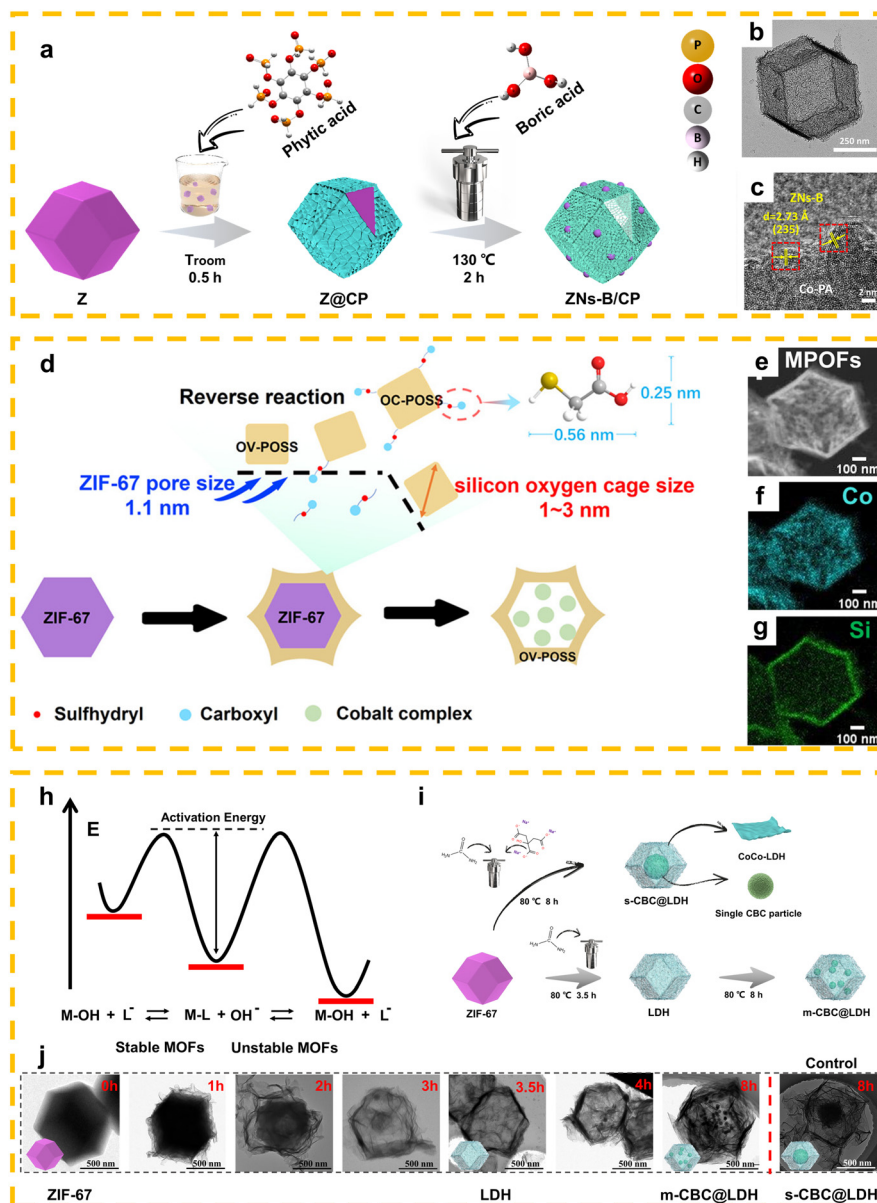


**Fig. 2** (a) A schematic of the synthesis of ZNs-B/CP; (b and c) TEM image and HRTEM image of ZNs-B/CP. Reproduced from ref. 39 with permission from Elsevier, copyright 2022. (d) A schematic illustration of the hypothesized synthesis mechanism of the MPOFs; (e–g) TEM and elemental mapping (Co and Si) of MPOFs. Reproduced from ref. 41 with permission from the American Chemical Society, copyright 2022. (h) A schematic representation of the decomposition of MOFs under basic conditions (secondary production based on the original figure). Reproduced from ref. 44 with permission from the Royal Society of Chemistry, copyright 2022. (i) A schematic of the synthesis of LDH, m-CBC@LDH, and s-CBC@LDH; (j) TEM images of ZIF-67 treated with urea only with different reaction times, and the TEM image of ZIF-67 treated with urea and sodium citrate for 8 h (the inset in (j) shows the corresponding schematic). Reproduced from ref. 27 with permission from Elsevier, copyright 2023.

the coordination bonds for MOFs under alkaline conditions is simplified as a ligand exchange process, during which the coordination groups are substituted by anions/molecules in solution, such as  $OH^-$  and  $H_2O$ . Thermodynamically, MOFs are more inclined to keep a crystalline state if the coordination bond between the metal ion and the ligand (M–L) is stronger compared to that with  $OH^-$  or other coordinating anions (Fig. 2h).<sup>44</sup> Except for the binding capacity of the M–L bond, the thermodynamic stability of the final products that are formed by metal ions under alkaline

conditions should also be taken into account. Theoretically, a higher  $pK_{sp}$  indicates a greater affinity of metal ions for  $OH^-$ , which causes the MOFs composed of the corresponding metal ions to be more vulnerable in alkaline environments.<sup>45</sup>

Hu *et al.* synthesized covalent oxygen-rich  $C_2N$  (CNO) networks by microwave irradiation using HKUST-1 as a sacrificial template and urea as an etchant.<sup>46</sup> At only 2.0 wt% loading, the tensile and impact strengths of the as-prepared composites were increased by more than 36% compared with pure poly(lactic acid) (PLA), and the flame retardancy was





also appreciably improved. Moreover, we prepared a series of nanocages with different micro-nanostructures, *i.e.*, hollow, yolk@shell, and multi-yolk@shell, using ZIF-67 as the precursor and urea as the etchant (Fig. 2i and j).<sup>27</sup> It was found that this “nest-in-egg” like nanostructure has more obvious flame retardant advantages. This is mainly attributed to the fact that the nanoshells assembled from CoCo-LDH pre-catalyze the char formation of the matrix, while the inner cobalt basic carbonate (CBC) nanoparticles provide assisted charring, which efficiently mitigates the fire hazard.

## 2.4 Polycondensation

Extensive research has been conducted on core/shell nanostructured flame retardants. Nevertheless, the available yolk@shell flame retardants can be counted on one's fingers. This is mainly due to the difficult-to-regulate synthesis process of this particular structure.<sup>47</sup> The yolk@shell structure is suggested to have superior mass transfer capability and catalytic properties.<sup>48</sup>

Motivated by the coating strategy and the acid etching strategy, our group reported for the first time the simultaneous coating treatment and etching for ZIF-67 by means of the phenomenon of acid generation from the condensation of specific compounds, so as to regulate the nanostructure, flame retardant performance, and compatibility.

The interface between the composite components acts as a critical role in the overall material properties, such as mechanical properties, glass transition temperature, aging, dielectric behavior, density, and flammability. Therefore, the filler dispersion and interfacial characteristics have to be considered for the structure–property–processing studies of polymer nanocomposites.<sup>21</sup> Our group obtained yolk-double shell structures (ZIF-67@layered double hydroxides@polyphosphazenes, ZIF@LDH@PZS), as well as hollow nanocages with treble shells as peculiar nanostructures (LDH@PZS@NH) by further etching of polyphosphoronitrile-coated ZIF-67 to different degrees (Fig. 3a–d), respectively. We found that the different outer

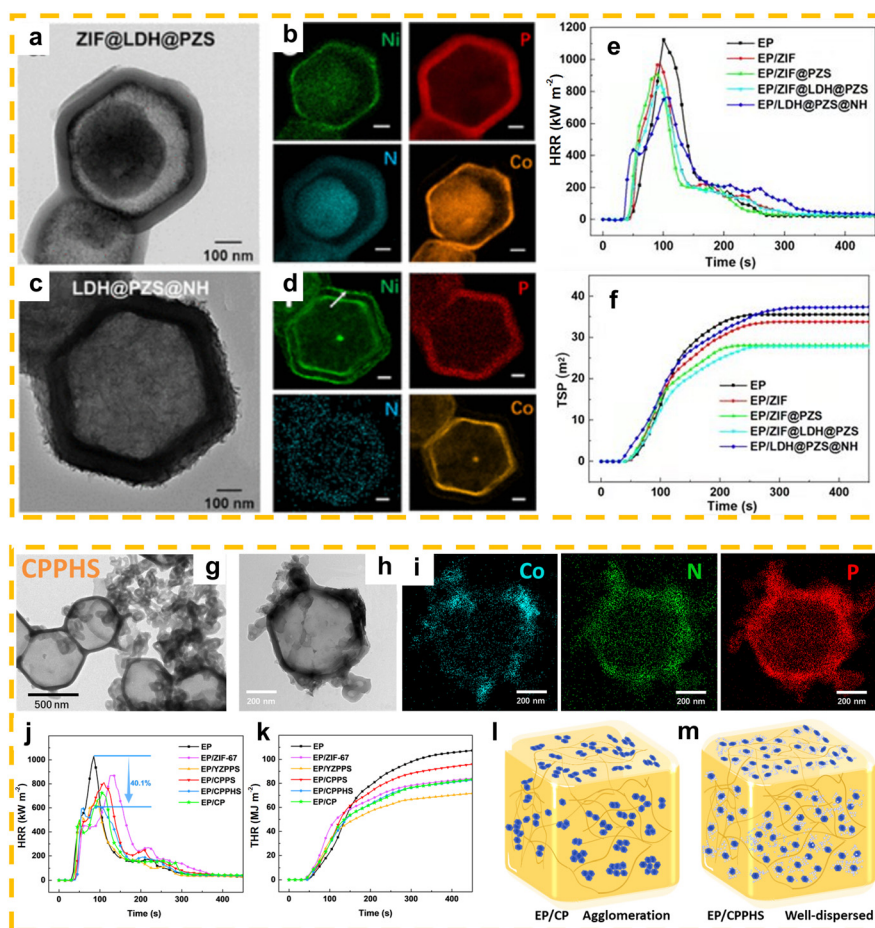


**Fig. 3** (a and c) The TEM images and (b and d) elemental mappings (scale bar: 100 nm) of ZIF@LDH@PZS and LDH@PZS@NH, respectively; (e and f) HRR and TSP curves of epoxy and its composites. Reproduced from ref. 49 with permission from the American Chemical Society, copyright 2022. (g–i) TEM image, enlarged TEM image, and elemental mapping (Co, N, and P) of CPPHS; (j and k) HRR and THR curves for epoxy and its composites; (l and m) presumed dispersion mechanism of CP and CPPHS in the epoxy matrix. Reproduced from ref. 50 with permission from Elsevier, copyright 2023.



layers of the hybrids conferred different interfacial interactions within the epoxy group. The influence of the interfacial relationship between the hybrids and the polymers on the comprehensive performance of the composites was explored by tuning the surface structure of the hybrids. Compared to the ZIF@LDH@PZS, the LDH@PZS@NH presented inferior compatibility due to the outer nickel hydroxide nanosheets hindering the interfacial interaction between the polyphosphoronitrile and the matrix, and the poor modification effect caused was verified by the flame retardancy and mechanical properties analysis of the epoxy nanocomposites (Fig. 3e and f).<sup>49</sup> Subsequently, using ZIF-67 and cobalt compounds derived from cobalt ions released from ZIF-67 as double templates involved in the nucleation process of polyphosphoronitrile, our group ingeniously synthesized a polyphosphoronitrile hollow hybrid material, which consisted of polyphosphoronitrile hollow nanospheres (PHNSs), as well as cobalt-doped polyphosphoronitrile hollow sub-micron polyhedra (CPs) with different sizes and dimensions (Fig. 3g-i).<sup>50</sup> The as-prepared fillers not only imparted excellent flame-retardant properties to the epoxy composites (Fig. 3j and k), but also improved the mechanical properties significantly. Due to the size difference of an order of magnitude between the 0D PHNSs and 3D CPs contained in the as-prepared filler, the contact area between them is relatively small. The PHNSs dispersed around the CPs is analogous to the sliding beads in the bearings, which effectively attenuates the agglomeration between the CPs and facilitates their dispersion in the EP matrix (Fig. 3l and m).<sup>51,52</sup> This dimensional mismatch structure can effectively avoid the early fracture of the EP composites due to the excessive stress

caused by the local filler agglomeration during mechanical loading.<sup>53,54</sup>

### 3 Function of cleft MOFs and the application as FRs

#### 3.1 Endowing the synergist effect

Compared with traditional flame retardants, MOFs-based flame retardants exhibit exceptional properties in terms of chemical composition, nanostructure and porosity characteristics. They are also expected to be applied as synergists to improve the comprehensive performance of composites, while alleviating the shortcomings of the high-cost MOFs.<sup>55,56</sup> In addition, the introduction of commercial flame retardants into the polymer matrix often causes an inevitable loss on mechanical properties. MOFs-based flame retardants as synergists can significantly reduce the amount of commercial flame retardants, thus improving the mechanical properties of the composites. Recent published papers that focus on the function of cleft MOFs and the application as FRs are summarized in Table 2.

Piao *et al.* reported a flame-retardant polyurethane (PU) sponge (FPUF@MOF-LDH@HDTMS) based on a biomimetic structure for continuous oil-water separation and with a separation efficiency of up to 99.1%.<sup>57</sup> The conversion of anisotropic MOF-LDH (CuCo-LDH) was realized by etching ZIF-67 crystals grown *in situ* on the skeleton of the PU sponge. This significantly improves the roughness and surface area of the PU sponge, and facilitates efficient grafting of hexadecyltrimethoxysilane (HDTMS). They suggested that MOF-LDH@HDTMS, like the papillae on the

**Table 2** Summary of the flame-retardant properties of the function of cleft MOFs and the application as FRs

Polymer systems	Type of FRs	Loading (wt%)	Main flame-retardant results	Ref.
Polyurethane	MOF-LDH@HDTMS	—	30.3%, 20.6%, and 29.9% reduction in pHRR, SPR, and PCOPR (heat flux of 35 kW m <sup>-2</sup> )	57
E-44/DDM	NiCo-LDH@PZS	4.0	30.9% and 11.2% reduction in pHRR and THR (results of microscale combustion calorimeter)	32
E-44/m-phenylenedi-amine	ZIF-8@HCCP	4.0	47.1% and 21.8% reduction in pHRR and TSP (heat flux of 50 kW m <sup>-2</sup> ; 3 mm thickness)	68
E-44/DDS	TPP@LDH@Co-PDA	2.0	29.4% of LOI; 43.1% reduction in pHRR (heat flux of 50 kW m <sup>-2</sup> ; 3 mm thickness)	69
Polystyrene	Macroporous MIL-53 (T-Fe-MOF)	3.0	24.7%, 40.6% and 68.9% reduction in pHRR, PCOPR and PCO <sub>2</sub> PR (heat flux of 35 kW m <sup>-2</sup> )	70
Polyurea	m-CBC-P@LDH	5.0	22.6% of LOI; 41.6% and 20.6% reduction in pHRR and THR (heat flux of 50 kW m <sup>-2</sup> ; 3 mm thickness)	20
E-51/DDM	W-Zr-MOF-NH <sub>2</sub>	3.0	36.6% and 26.1% reduction in TSP and THR (heat flux of 35 kW m <sup>-2</sup> ; 3 mm thickness)	42
E-44/DDS	ZHS@NCH	6.0	UL-94 V-0 rating (3.2 mm thickness); 69.1% and 36.1% reduction in pHRR and TSP (heat flux of 50 kW m <sup>-2</sup> ; 3 mm thickness)	22
RIM935 epoxy/RIM936 hardener	P-UiO-66 NH <sub>2</sub>	1.0	UL-94 V-1 rating (3.2 mm thickness); 30.0%, 42.0%, and 43.0% reduction in pHRR, smoke production rate, and carbon monoxide emission (heat flux of 50 kW m <sup>-2</sup> ; 3 mm thickness)	83
E-51/DDM	W-Zr-MOF-DOPO	3.0	32.2% of LOI; UL-94 V-0 rating; 36.0% and 57.8% reduction in TSP and pHRR (heat flux of 35 kW m <sup>-2</sup> ; 3 mm thickness)	42
Epoxydhdraz C/DDM	PA-UiO66-NH <sub>2</sub>	5.0	41% and 42% reduction in the pHRR and TSP (heat flux of 50 kW m <sup>-2</sup> ; 3.2 mm thickness)	84
E-44/DDS	MPOFs-P	2.0	27.0% of LOI; UL-94 V-0 rating (3.2 mm thickness); 46.6% and 25.2% reduction in pHRR and TSP (heat flux of 50 kW m <sup>-2</sup> ; 3 mm thickness)	41





surface of the lotus flower, forms a multistage micro-nano structure consisting of hydrophilic protrusions and hydrophobic surfaces on the sponge surface. Meanwhile, MOF-LDH serves as a co-effector of the phosphorus nitrogen-functionalized lignocellulosic fiber flame-retardant coating (LFPN) to endow the composites with outstanding flame retardancy, as well as smoke and toxic gas inhibition. LFPN undergoes phosphate esterification during decomposition to facilitate matrix dehydration towards char, while CuCo-LDH decomposes to produce oxides (e.g.,  $\text{Cu}_2\text{O}$ ,  $\text{CuO}$ ,  $\text{CoO}$ ,  $\text{Co}_3\text{O}_4$ , etc.), which synergistically boosts the yield and antioxidant capacity of the coke layer. In addition, copper ions can cause the catalytic conversion of  $\text{CO}$  to  $\text{CO}_2$  via the Mars-van Krevelen mechanism to diminish the  $\text{CO}$  emission.<sup>28,58</sup>

To improve the compatibility of LDHs to enhance their fire safety in epoxy composites, Hu *et al.* synthesized hollow dodecahedral NiCo-LDH@PZS with ZIF-67 as a precursor and a sacrificial template, and polyphosphazene (PZS) as an interface compatibilizer and flame retardant.<sup>32</sup> PZS has excellent free radical trapping capacity as well as char formation effect, and synergies with NiCo-LDH significantly inhibit the smoke toxicity generated during the combustion process of EP composites and promote the formation of graphitized residual char. The storage modulus and glass transition temperature of the modified EP composites were enhanced. This is mainly attributed to the enhanced interaction and compatibility between NiCo-LDH@PZS and epoxy molecular chains, which hinders the movement of molecular chains. Moreover, the interface between the rough nano-surface of the filler and the organic phase can transfer most of the energy under an external load.

### 3.2 Pore structure engineering

Surprisingly, defective MOFs are more prevalent in the synthesis process, and they often exhibit unexpected high performance in different applications (e.g., adsorption, catalysis, and magnetism, etc.) compared to perfect MOFs crystals, thanks to the enhanced porosity and rich active site generation.<sup>59–63</sup> As a porous material, MOFs can adsorb smoke particles and toxic gases generated by polymers during combustion. Nevertheless, the single use of MOFs as a flame retardant filler is often hampered by the insufficient charring ability capacity. The loading of functional fillers is an effective strategy to solve this challenge. Removal of the central atom or ligand can create defects by cleaving the metal-ligand coordination bond. If the cleavage area or ligand size is increased, hierarchical pores are created, which facilitates the diffusion of larger molecules.<sup>64–67</sup>

**3.2.1 Phosphorus-containing small molecule flame retardants loading.** There has been much focus on the development and application of phosphorus-containing small molecule flame retardants (P-FRs) as efficient halogen-free flame retardants due to their low toxicity, high flame retardant efficiency and designability. However, the migration precipitation problems and plasticizing polymer

molecular chains remain as challenges that seriously impair the flame retardancy and mechanical properties of the composites. The strategy of exploiting MOFs-based carriers to avoid the migration of small-molecule P-FRs is considered to be a promising solution to the above problems, but only a few studies have been conducted. Currently, the dominant methods are classified as *in situ* synthesis and post-synthesis modification.

Meng *et al.* successfully encapsulated hexachlorocyclotriphosphazene (HCCP) within the framework of ZIF-8 by taking advantage of its small-window and large-pore feature, and the thermal stability of the as-prepared filler could be regulated by the encapsulation amount.<sup>68</sup> Our group also adopted the bottom-up method to encapsulate triphenyl phosphate (TPP), a phosphorus flame retardant, in the LDHs nanocages derived from ZIF-67, and further modified the surface by poly-dopamine (PDA) to improve the thermal stability and compatibility of LDHs, while inhibiting the migration problem of the phosphorus small molecules.<sup>69</sup> However, there are still restrictions on the universality of this method. If there are too many flame-retardant guests involved or the size of the flame-retardant guests is too large, this may destroy the original coordination environment and even trigger the instability of the crystal structure. Thus, the choice of the appropriate guest is essential.

Post-synthesis modification methods possess a more advantageous designability compared to *in situ* synthesis methods. Efficient loading of the guest can be accomplished by defect engineering strategies to prepare carriers with hierarchical porous or hollow structures. Zhao *et al.*<sup>70</sup> prepared macroporous iron-metal-organic frameworks (MIL-53(Fe)) loaded with triethyl phosphate using an aqueous ammonia solution as an etchant. Compared with pure polystyrene, the pHRR, THR and peak  $\text{CO}$  production rate of the composites doped with 3.0 wt% filler decreased by 24.7%, 12.7%, and 40.7%, respectively, and the smoke density ranking also decreased by 26.1%. Recently, our group constructed bird's nest-like hierarchical porous nanocages to achieve the effective loading of triphenyl phosphate up to 35.8 wt% (Fig. 4a–c). The as-prepared composites showed good durability in terms of their flame-retardant properties.<sup>20</sup> It should be noted that phosphorus-containing flame retardants with a single structure have a common disadvantage: they rarely affect the oxidation of poisonous gases during polymer combustion. Furthermore, transition metal compounds (such as Fe, Co and Ni) have been widely studied in many fields owing to their excellent catalytic oxidation properties.<sup>71</sup> Therefore, the combination of phosphorus-containing flame retardants and MOFs-based flame retardants has been shown to eliminate this shortcoming.

**3.2.2 Combustion volatiles capture.** Considering that the smoke generated during polymer combustion is generally incomplete combustion volatiles, the particle size is too large to be captured by the micropores of MOFs.<sup>72–75</sup> So far, metal-organic frameworks with open nanostructures have been proven to have excellent capture capacity for smoke particles compared to solid MOFs.<sup>76,77</sup> However, the exploration and



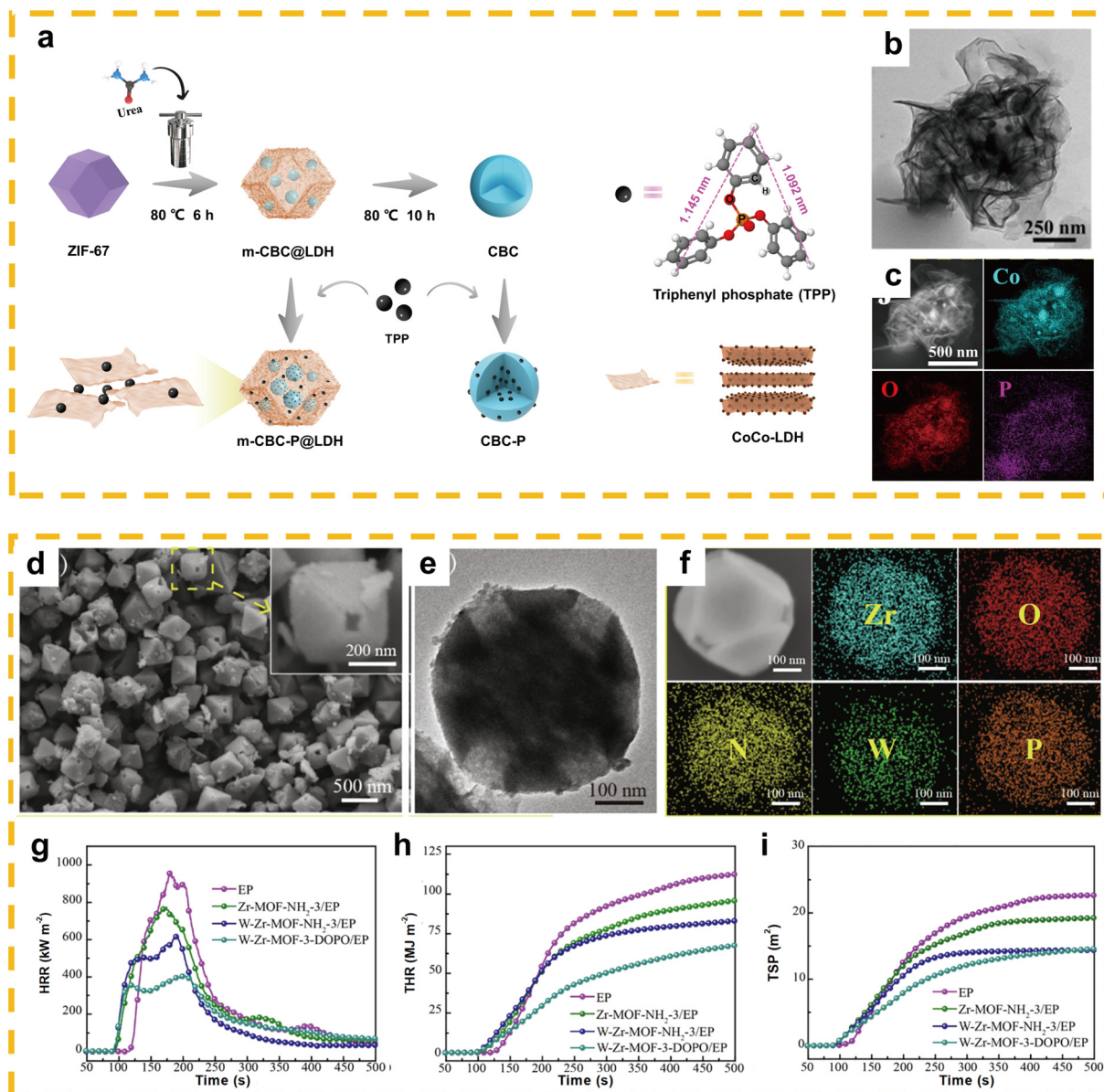


**Fig. 4** (a) A schematic illustration of the preparation of m-CBC@LDH, m-CBC-P@LDH, CBC and CBC-P; (b and c) TEM image and the corresponding elemental mapping images of m-CBC-P@LDH. Reproduced from ref. 20 with permission from Academic Press Inc, copyright 2023; (d) SEM image, (e) TEM image, and (f) element mapping images of W-Zr-MOF-3-DOPO; (g-i) HRR, THR, and TSP curves of EP and its composites. Reproduced from ref. 42 with permission from Elsevier, copyright 2021.

design of hierarchical porous materials derived from MOFs has remained a great challenge. To date, only a few MOF-based strategies have been reported for the synthesis of open cages, which are mainly restricted to wet-chemistry liquid methods for fabricating predesigned MOF structures.<sup>78–80</sup>

Dai *et al.* reported on hierarchical porous bimetallic organic frameworks (W-Zr-MOF-NH<sub>2</sub>) using Zr-MOF-NH<sub>2</sub> as a template through a metal-acid-assisted etching method.<sup>42</sup> Compared to the compact (111) crystal plane of the Zr-MOF-NH<sub>2</sub> structure, the (100) crystal plane is rich in regular pores, so the six (100) crystal planes of Zr-MOF-NH<sub>2</sub> are preferentially etched to form a unique elongated channel structure (Fig. 4d–f). This hierarchical porous structure

effectively promotes the adsorption and catalytic charring of pyrolytic volatiles. Thus, the TSP and THR of the epoxy composites with only 3.0 wt% W-Zr-MOF-NH<sub>2</sub> were significantly reduced by 36.6% and 26.1%, respectively, compared to the pure epoxy resin (Fig. 4g–i).

### 3.3 Morphological regulation

MOFs-derived hollow structures, yolk@shell structures, and laminated structures expose more active sites, as well as faster mass transport through complete or incomplete conversion compared to bulk MOFs.<sup>81,82</sup> Such peculiar structures can be fabricated by either transition metal salt



etching or acid/base etching strategies under certain reaction conditions, and the detailed principles have been elaborated as above. Flame retardants with single yolk@shell structures and multi-yolk@shell structures are rarely reported in the flame retardant field due to their sophisticated synthesis. Our group constructed several representative ZIF-67-derived flame retardants with yolk-shell structures *via* one-pot, top-down, and bottom-up strategies.<sup>8,27,49</sup> Typically, in order to avoid agglomeration of nanoparticles on the carriers and prevent the “second agglomeration” caused by nanoparticles falling off the carriers, our group prepared the multi-yolk@shell nanostructured hybrid flame retardant ZHS@NCH by using the self-template and ion exchange strategy.<sup>22</sup> Zinc hydroxystannate (ZHS) is uniformly and restrictively dispersed in the cavity of the layered bimetallic (Ni-Co) hydroxide nanocages (NCH) derived from ZIF-67. Compared with pure ZHS, pure NCH and physical mixture of ZHS and NCH, the epoxy nanocomposites mixed with ZHS@NCH have better flame retardancy and mechanical properties.

### 3.4 Gifting multifunctionality

The easy functionalization of MOFs also creates convenient conditions for grafting target molecules. The main methods include the substitution reaction between amino-functionalized MOFs and flame retardants containing phosphorus-chlorine bonds; the addition reaction between double-bond functionalized MOFs and flame retardants containing phosphorus-hydrogen bonds; and the salt-forming reaction between amino-functionalized MOFs and flame retardants containing phosphate ester bonds.<sup>8</sup>

Vishnu Unnikrishnan *et al.* synthesized an organophosphorus-functionalized zirconium-based MOF, which effectively improved the mechanical properties and fire safety of epoxy composites.<sup>83</sup> Compared to the pure epoxy resin, the epoxy composites mixed with 1.0 wt% filler showed 13.8% and 28.8% increase in tensile and flexural strengths, as well as 30%, 42%, and 43% reduction in pHRR, SPR, and carbon monoxide emission, respectively.

Dai *et al.* reported on organophosphorus modified hollow bimetallic organic frameworks (W-Zr-MOF-DOPO) with hierarchical porosity.<sup>42</sup> Only 3.0 wt% addition of W-Zr-MOF-DOPO can impart the epoxy composite with 32.2% LOI value and pass the UL-94 V-0 rating. In addition, the pHRR and TSP of the epoxy composites were significantly reduced by 57.8% and 36.1%, respectively, compared to the pure epoxy. Similarly, Wang *et al.* synthesized a phosphorus-rich metal-organic framework *via* amino-carrying zirconium-based MOFs interacting with bio-based phytic acid, and significantly improved the flame-retardant properties and smoke-toxicity suppression of the epoxy composites.<sup>84</sup>

Our group obtained MOFs containing double bonds by etching ZIF-67 with carboxyl-functionalized POSS, and further added a small molecular phosphorus flame retardant.<sup>41</sup> The as-prepared fillers (MPOFs-P) integrating transition metals,

silicon and phosphorus endowed the epoxy composites with a limiting oxygen index of 25.0% and passed the UL-94 V-0 rating at only 2.0 wt% loading. In addition, the pHRR and TSP are reduced by 46.6% and 25.2%, respectively, relative to the pure epoxy resin. This work sheds light on the preparation of efficient multi-element flame-retardant systems by hybridization methods of MOFs and POSS.

## 4 Summary and outlook

Based on the above reports on the cleft MOFs in polymeric materials, we provide a brief summary here. (1) Cleft MOFs can be used in conjunction with other commercial flame retardants to achieve higher flame-retardant efficiency and mechanical enhancement at lower loadings; (2) the combination of cleft MOFs and 2D materials can improve the dispersion state of the filler in the matrix, and significantly inhibit the heat release and smoke release of the composite; (3) there are abundant active sites on the surface of MOFs, which facilitate their modification by functional components. MOFs in combination with phosphorus-containing components typically exhibit enhanced flame retardancy, and are more likely to achieve higher ratings in the vertical burning tests; (4) due to their inherent porous structure, MOFs-derived carriers are more advantageous, accompanied by higher small molecule flame retardant loading, compared to chemical grafting and capillary adsorption; (5) compared with microporous MOFs, hierarchical porous MOFs derivatives are particularly advantageous in terms of their smoke capture ability.

Metal-organic frameworks-derived flame retardants have emerged as an emerging class of additives in polymeric materials with outstanding flame-retardant advantages. MOFs-based flame retardants possess fascinating features in terms of their tailored chemical composition, tunable nanostructure, and abundant porosity compared to conventional flame retardants. Herein, a comprehensive review of different methods of MOFs cleavage for flame retardant applications is presented.

Although the current research on MOFs-based flame retardants has achieved stage-by-stage results, there is still a gap from industrial application, and the following problems still need to be further explored and solved.

(1) Although there are some commercialized MOFs, the high cost remains a major constraint on MOFs-based FRs that cannot be ignored. There is also an urgent need to establish a systematic cost evaluation system for MOFs, *i.e.*, to consider a comprehensive range of process parameters, such as scale, raw materials, and the costs of recycling and washing;

(2) To explore the composite system of MOFs and their derivatives as synergists with commercial flame retardants for improving the deficiencies of composites in mechanical, flame retardant and smoke inhibition properties;

(3) Endowing MOFs-based flame retardants with multifunctionality (*e.g.*, composites that are both flame-





retardant and phase change composites, composites that are both flame-retardant and electromagnetically shielded, *etc.*) to compensate for their high cost;

(4) For the selection of ligands, the design of flame-retardant ligands or bio-based ligands can be considered for the improvement of the flame-retardant capability of MOFs, as well as cost reduction;

(5) The high cost of MOFs is inextricably linked to expensive ligands. Thus, the development of suitable ligand recovery strategies is also a challenge that needs to be urgently addressed.

## Abbreviations

SEM	Scanning electron microscope
TEM	Transmission electron microscope
HRTEM	High-resolution transmission electron microscope
ZIF@LDH@PZS	ZIF-67@layered double hydroxides@polyphosphazenes
LDH@PZS@NH	ZIF-67@layered double hydroxides@Ni(OH) <sub>2</sub>
DDS	Diaminodiphenyl sulfone
DDM	Diaminodiphenyl methane
m-CBC@LDH	Multi-yolk@shell cobalt basic carbonate@CoCo-LDH
m-CBC-P@LDH	Triphenyl phosphate-loaded multi-yolk@shell cobalt basic carbonate@CoCo-LDH
CBC	Cobalt basic carbonate
CBC-P	Triphenyl phosphate-loaded cobalt basic carbonate

## Author contributions

The manuscript was written through contributions of all authors. CRediT: Kunpeng Song conceptualization, formal analysis, data curation, investigation, methodology, visualization, writing – original draft, writing – review & editing; Ye-Tang Pan supervision, validation, funding acquisition, resources, writing – review & editing; Jiyu He funding acquisition, validation, supervision, writing – review & editing, project administration; Rongjie Yang funding acquisition, validation, supervision, resources.

## Conflicts of interest

The authors declare that they have no known competing financial interests or personal relationships that could have appeared to influence the work reported in this paper.

## Acknowledgements

This work was supported by the National Natural Science Foundation of China (No. 22005029 and 22375023) and the BIT Research and Innovation Promoting Project (Grant No. 2023YCX041).

## References

- 1 Y. Qian, F. Zhang and H. Pang, A review of MOFs and their composites-based photocatalysts: Synthesis and applications, *Adv. Funct. Mater.*, 2021, **31**, 2104231.
- 2 M. Ahmed, Recent advancement in bimetallic metal organic frameworks (M<sup>2</sup>MOFs): Synthetic challenges and applications, *Inorg. Chem. Front.*, 2022, **9**, 3003–3033.
- 3 C. Li, H. Zhang, M. Liu, F.-F. Lang, J. Pang and X.-H. Bu, Recent progress in metal–organic frameworks (MOFs) for electrocatalysis, *Ind. Chem. Mater.*, 2023, **1**, 9–38.
- 4 Y. Dai, G. Zhang, Y. Peng, Y. Li, H. Chi and H. Pang, Recent progress in 1D MOFs and their applications in energy and environmental fields, *Adv. Colloid Interface Sci.*, 2023, **321**, 103022.
- 5 J. Zhang, Z. Li, X.-L. Qi and D.-Y. Wang, Recent progress on metal–organic framework and its derivatives as novel fire retardants to polymeric materials, *Nano-Micro Lett.*, 2020, **12**, 173.
- 6 Y. Hou, W. Hu, Z. Gui and Y. Hu, Preparation of metal–organic frameworks and their application as flame retardants for polystyrene, *Ind. Eng. Chem. Res.*, 2017, **56**, 2036–2045.
- 7 Y.-T. Pan, Z. Zhang and R. Yang, The rise of MOFs and their derivatives for flame retardant polymeric materials: A critical review, *Composites, Part B*, 2020, **199**, 108265.
- 8 K. Song, Y.-T. Pan, J. Zhang, P. Song, J. He, D.-Y. Wang and R. Yang, Metal–organic frameworks–based flame-retardant system for epoxy resin: A review and prospect, *Chem. Eng. J.*, 2023, **468**, 143653.
- 9 H. Nabipour, X. Wang, L. Song and Y. Hu, Metal–organic frameworks for flame retardant polymers application: A critical review, *Composites, Part A*, 2020, **139**, 106113.
- 10 R. Kumar, M. Mooste, Z. Ahmed, S. Akula, I. Zekker, M. Marandi, M. Käärrik, J. Leis, A. Kikas, A. Treshchalov, M. Otsus, J. Aruväli, V. Kisand, A. Tamm and K. Tammeveski, Highly active ZIF-8@CNT composite catalysts as cathode materials for anion exchange membrane fuel cells, *Ind. Chem. Mater.*, 2023, **1**, 526–541.
- 11 N. Talukder, Y. Wang, B. B. Nunna, X. Tong, J. A. Boscoboinik and E. S. Lee, Investigation on electrocatalytic performance and material degradation of an N-doped graphene-MOF nanocatalyst in emulated electrochemical environments, *Ind. Chem. Mater.*, 2023, **1**, 360–375.
- 12 L. Jiao, J. Y. R. Seow, W. S. Skinner, Z. U. Wang and H.-L. Jiang, Metal–organic frameworks: Structures and functional applications, *Mater. Today*, 2019, **27**, 43–68.
- 13 R. E. Morris and J. Čejka, Exploiting chemically selective weakness in solids as a route to new porous materials, *Nat. Chem.*, 2015, **7**, 381–388.
- 14 X. Zhou, H. Jin, B. Y. Xia, K. Davey, Y. Zheng and S.-Z. Qiao, Molecular cleavage of metal–organic frameworks and application to energy storage and conversion, *Adv. Mater.*, 2021, **33**, 2104341.



- 15 G. Wang, D. Huang, M. Cheng, S. Chen, G. Zhang, L. Lei, Y. Chen, L. Du, R. Li and Y. Liu, Metal-organic frameworks template-directed growth of layered double hydroxides: A fantastic conversion of functional materials, *Coord. Chem. Rev.*, 2022, **460**, 214467.
- 16 S. Sanati, A. Morsali and H. García, First-row transition metal-based materials derived from bimetallic metal-organic frameworks as highly efficient electrocatalysts for electrochemical water splitting, *Energy Environ. Sci.*, 2022, **15**, 3119–3151.
- 17 H. Liu, M. Cheng, Y. Liu, J. Wang, G. Zhang, L. Li, L. Du, G. Wang, S. Yang and X. Wang, Single atoms meet metal-organic frameworks: Collaborative efforts for efficient photocatalysis, *Energy Environ. Sci.*, 2022, **15**, 3722–3749.
- 18 Y.-T. Pan, L. Zhang, X. Zhao and D.-Y. Wang, Interfacial engineering of renewable metal organic framework derived honeycomb-like nanoporous aluminum hydroxide with tunable porosity, *Chem. Sci.*, 2017, **8**, 3399–3409.
- 19 Z. Jiang, Z. Li, Z. Qin, H. Sun, X. Jiao and D. Chen, LDH nanocages synthesized with MOF templates and their high performance as supercapacitors, *Nanoscale*, 2013, **5**, 11770–11775.
- 20 K. Song, H. Zhang, Y.-T. Pan, Z. Ur Rehman, J. He, D.-Y. Wang and R. Yang, Metal-organic framework-derived bird's nest-like capsules for phosphorous small molecules towards flame retardant polyurea composites, *J. Colloid Interface Sci.*, 2023, **643**, 489–501.
- 21 M. Zammarano, M. Franceschi, S. Bellayer, J. W. Gilman and S. Meriani, Preparation and flame resistance properties of revolutionary self-extinguishing epoxy nanocomposites based on layered double hydroxides, *Polymer*, 2005, **46**, 9314–9328.
- 22 Z. Zhang, X. Li, Y. Yuan, Y.-T. Pan, D.-Y. Wang and R. Yang, Confined dispersion of zinc hydroxystannate nanoparticles into layered bimetallic hydroxide nanocapsules and its application in flame-retardant epoxy nanocomposites, *ACS Appl. Mater. Interfaces*, 2019, **11**, 40951–40960.
- 23 A. Dasari, Z.-Z. Yu, G.-P. Cai and Y.-W. Mai, Recent developments in the fire retardancy of polymeric materials, *Prog. Polym. Sci.*, 2013, **38**, 1357–1387.
- 24 C. Nyambo, E. Kandare and C. A. Wilkie, Thermal stability and flammability characteristics of ethylene vinyl acetate (EVA) composites blended with a phenyl phosphonate-intercalated layered double hydroxide (LDH), melamine polyphosphate and/or boric acid, *Polym. Degrad. Stab.*, 2009, **94**, 513–520.
- 25 X.-H. Shi, X.-L. Li, Q.-Y. Liu, S.-J. Wu, W.-M. Xie, N. Zhao, J. De La Vega, M.-J. Chen and D.-Y. Wang, Constructing Co-decorated layered double hydroxide via interfacial assembly and its application in flame-retardant epoxy resin, *Compos. Commun.*, 2023, **43**, 101712.
- 26 Z. Li, J. Wang, D. F. Expósito, J. Zhang, C. Fu, D. Shi and D.-Y. Wang, High-performance carrageenan film based on carrageenan intercalated layered double hydroxide with enhanced properties: Fire safety, thermal stability and barrier effect, *Compos. Commun.*, 2018, **9**, 1–5.
- 27 K. Song, X. Li, Y.-T. Pan, B. Hou, Z. U. Rehman, J. He and R. Yang, The influence on flame retardant epoxy composites by a bird's nest-like structure of Co-based isomers evolved from zeolitic imidazolate framework-67, *Polym. Degrad. Stab.*, 2023, **211**, 110318.
- 28 Y. Qian, W. Su, L. Li, R. Zhao, H. Fu, J. Li, P. Zhang, Q. Guo and J. Ma, Cooperative effect of ZIF-67-derived hollow NiCo-LDH and MoS<sub>2</sub> on enhancing the flame retardancy of thermoplastic polyurethane, *Polymers*, 2022, **14**, 2204.
- 29 Y.-T. Pan, J. Wan, X. Zhao, C. Li and D.-Y. Wang, Interfacial growth of MOF-derived layered double hydroxide nanosheets on graphene slab towards fabrication of multifunctional epoxy nanocomposites, *Chem. Eng. J.*, 2017, **330**, 1222–1231.
- 30 Y. Hou, S. Qiu, Y. Hu, C. K. Kundu, Z. Gui and W. Hu, Construction of bimetallic ZIF-derived Co-Ni LDHs on the surfaces of GO or CNTs with a recyclable method: Toward reduced toxicity of gaseous thermal decomposition products of unsaturated polyester resin, *ACS Appl. Mater. Interfaces*, 2018, **10**, 18359–18371.
- 31 Z. Zhang, J. Qin, W. Zhang, Y.-T. Pan, D.-Y. Wang and R. Yang, Synthesis of a novel dual layered double hydroxide hybrid nanomaterial and its application in epoxy nanocomposites, *Chem. Eng. J.*, 2020, **381**, 122777.
- 32 X. Zhou, X. Mu, W. Cai, J. Wang, F. Chu, Z. Xu, L. Song, W. Xing and Y. Hu, Design of hierarchical NiCo-LDH@PZS hollow dodecahedron architecture and application in high-performance epoxy resin with excellent fire safety, *ACS Appl. Mater. Interfaces*, 2019, **11**, 41736–41749.
- 33 Z.-H. Wang, B.-W. Liu, F.-R. Zeng, X.-C. Lin, J.-Y. Zhang, X.-L. Wang, Y.-Z. Wang and H.-B. Zhao, Fully recyclable multifunctional adhesive with high durability, transparency, flame retardancy, and harsh-environment resistance, *Sci. Adv.*, 2022, **8**, eadd8527.
- 34 W. Rao, J. Tao, F. Yang, T. Wu, C. Yu and H.-B. Zhao, Growth of copper organophosphate nanosheets on graphene oxide to improve fire safety and mechanical strength of epoxy resins, *Chemosphere*, 2023, **311**, 137047.
- 35 L. Zhang, S. Chen, Y.-T. Pan, S. Zhang, S. Nie, P. Wei, X. Zhang, R. Wang and D.-Y. Wang, Nickel metal-organic framework derived hierarchically mesoporous nickel phosphate toward smoke suppression and mechanical enhancement of intumescent flame retardant wood fiber/poly(lactic acid) composites, *ACS Sustainable Chem. Eng.*, 2019, **7**, 9272–9280.
- 36 S. Zheng, Y. Sun, H. Xue, P. Braunstein, W. Huang and H. Pang, Dual-ligand and hard-soft-acid-base strategies to optimize metal-organic framework nanocrystals for stable electrochemical cycling performance, *Natl. Sci. Rev.*, 2021, **9**, nwab197.
- 37 P. Yang, F. Mao, Y. Li, Q. Zhuang and J. Gu, Hierarchical porous Zr-based MOFs synthesized by a facile monocarboxylic acid etching strategy, *Chem. – Eur. J.*, 2018, **24**, 2962–2970.
- 38 J. Koo, I.-C. Hwang, X. Yu, S. Saha, Y. Kim and K. Kim, Hollowing out MOFs: Hierarchical micro-and mesoporous MOFs with tailorable porosity via selective acid etching, *Chem. Sci.*, 2017, **8**, 6799–6803.



- 39 K. Song, B. Hou, Z. Ur Rehman, Y.-T. Pan, J. He, D.-Y. Wang and R. Yang, "Sloughing" of metal-organic framework retaining nanodots via step-by-step carving and its flame-retardant effect in epoxy resin, *Chem. Eng. J.*, 2022, **448**, 137666.
- 40 H. Wang, X. Li, F. Su, J. Xie, Y. Xin, W. Zhang, C. Liu, D. Yao and Y. Zheng, Core-shell ZIF67@ZIF8 modified with phytic acid as an effective flame retardant for improving the fire safety of epoxy resins, *ACS Omega*, 2022, **7**, 21664–21674.
- 41 B. Hou, W. Zhang, H. Lu, K. Song, Z. Geng, X. Ye, Y.-T. Pan, W. Zhang and R. Yang, Multielement flame-retardant system constructed with metal-organic frameworks for epoxy resin, *ACS Appl. Mater. Interfaces*, 2022, **14**, 49326–49337.
- 42 X. Wang, T. Wu, J. Hong, J. Dai, Z. Lu, C. Yang, C. Yuan and L. Dai, Organophosphorus modified hollow bimetallic organic frameworks: Effective adsorption and catalytic charring of pyrolytic volatiles, *Chem. Eng. J.*, 2021, **421**, 129697.
- 43 K. Wang, X.-L. Lv, D. Feng, J. Li, S. Chen, J. Sun, L. Song, Y. Xie, J.-R. Li and H.-C. Zhou, Pyrazolate-based porphyrinic metal-organic framework with extraordinary base-resistance, *J. Am. Chem. Soc.*, 2016, **138**, 914–919.
- 44 K. Wang, Y. Li, L.-H. Xie, X. Li and J.-R. Li, Construction and application of base-stable MOFs: A critical review, *Chem. Soc. Rev.*, 2022, **51**, 6417–6441.
- 45 X.-L. Lv, K. Wang, B. Wang, J. Su, X. Zou, Y. Xie, J.-R. Li and H.-C. Zhou, A base-resistant metalloporphyrin metal-organic framework for C–H bond halogenation, *J. Am. Chem. Soc.*, 2017, **139**, 211–217.
- 46 Y. Hou, F. Chu, S. Ma, Y. Hu, W. Hu and Z. Gui, Rapid synthesis of oxygen-rich covalent C<sub>2</sub>N (CNO) nanosheets by sacrifice of HKUST-1: Advanced metal-free nanofillers for polymers, *ACS Appl. Mater. Interfaces*, 2018, **10**, 32688–32697.
- 47 X. Jiang, F. Chu, W. Liu, Y. Hu, W. Hu and L. Song, An individualized core-shell architecture derived from covalent triazine frameworks: Toward enhancing the flame retardancy, smoke release suppression, and toughness of bismaleimide resin, *ACS Mater. Lett.*, 2023, **5**, 630–637.
- 48 H. Chen, K. Shen, Q. Mao, J. Chen and Y. Li, Nanoreactor of MOF-derived yolk-shell Co@C–N: Precisely controllable structure and enhanced catalytic activity, *ACS Catal.*, 2018, **8**, 1417–1426.
- 49 B. Hou, K. Song, Z. Ur Rehman, T. Song, T. Lin, W. Zhang, Y.-T. Pan and R. Yang, Precise control of a yolk-double shell metal-organic framework-based nanostructure provides enhanced fire safety for epoxy nanocomposites, *ACS Appl. Mater. Interfaces*, 2022, **14**, 14805–14816.
- 50 X. Song, B. Hou, Z. Han, Y.-T. Pan, Z. Geng, L. H. Ibarra and R. Yang, Dual nucleation sites induced by ZIF-67 towards mismatch of polyphosphazene hollow sub-micron polyhedrons and nanospheres in flame retardant epoxy matrix, *Chem. Eng. J.*, 2023, **470**, 144278.
- 51 K. Song, Q. Li, Y. Yuan, S. Hu, J. Liu, Y. Zhang, Y.-T. Pan, W. Zhao and J. He, Hollow nanospheres of red phosphorus for fireproof flexible sensors fabricated via 3D printing, *ACS Appl. Nano Mater.*, 2022, **5**, 18080–18092.
- 52 H. Gu, J. Guo, H. Wei, S. Guo, J. Liu, Y. Huang, M. A. Khan, X. Wang, D. P. Young, S. Wei and Z. Guo, Strengthened magnetoresistive epoxy nanocomposite papers derived from synergistic nanomagnetite-carbon nanofiber nanohybrids, *Adv. Mater.*, 2015, **27**, 6277–6282.
- 53 Y. Hou, Z. Xu, R. An, H. Zheng, W. Hu and K. Zhou, Recent progress in black phosphorus nanosheets for improving the fire safety of polymer nanocomposites, *Composites, Part B*, 2023, **249**, 110404.
- 54 H. Zhao, Z. Yang and L. Guo, Nacre-inspired composites with different macroscopic dimensions: Strategies for improved mechanical performance and applications, *NPG Asia Mater.*, 2018, **10**, 1–22.
- 55 Y.-R. Li, Y.-M. Li, B.-B. Chen, W.-J. Hu and D.-Y. Wang, Highly efficient electromagnetic wave absorption Fe-MOF-rGO based composites with enhanced flame retardancy, *J. Alloys Compd.*, 2022, **918**, 165516.
- 56 G. Zhang, W. Wu, M. Yao, Z. Wu, Y. Jiao and H. Qu, Novel triazine-based metal-organic frameworks: Synthesis and multifunctional application of flame retardant, smoke suppression and toxic attenuation on EP, *Mater. Des.*, 2023, **226**, 111664.
- 57 J. Piao, M. Lu, J. Ren, Y. Wang, T. Feng, Y. Wang, C. Jiao, X. Chen and S. Kuang, MOF-derived LDH modified flame-retardant polyurethane sponge for high-performance oil-water separation: Interface engineering design based on bioinspiration, *J. Hazard. Mater.*, 2023, **444**, 130398.
- 58 Y. Zhou, S. Qiu, F. Chu, W. Yang, Y. Qiu, L. Qian, W. Hu and L. Song, High-performance flexible polyurethane foam based on hierarchical BN@MOF-LDH@APTES structure: Enhanced adsorption, mechanical and fire safety properties, *J. Colloid Interface Sci.*, 2022, **609**, 794–806.
- 59 S. Zhou, O. Shekhah, A. Ramírez, P. Lyu, E. Abou-Hamad, J. Jia, J. Li, P. M. Bhatt, Z. Huang, H. Jiang, T. Jin, G. Maurin, J. Gascon and M. Eddaoudi, Asymmetric pore windows in MOF membranes for natural gas valorization, *Nature*, 2022, **606**, 706–712.
- 60 Q. Hou, S. Zhou, Y. Wei, J. Caro and H. Wang, Balancing the grain boundary structure and the framework flexibility through bimetallic metal-organic framework (MOF) membranes for gas separation, *J. Am. Chem. Soc.*, 2020, **142**, 9582–9586.
- 61 X. Wang, Q. Lyu, T. Tong, K. Sun, L.-C. Lin, C. Y. Tang, F. Yang, M. D. Guiver, X. Quan and Y. Dong, Robust ultrathin nanoporous MOF membrane with intra-crystalline defects for fast water transport, *Nat. Commun.*, 2022, **13**, 266.
- 62 L.-L. Huang, L. Yu, B. Li, B.-B. Li, H. Wang and J. Li, Adsorption and release of 1-methylcyclopropene by metal-organic frameworks for fruit preservation, *ACS Mater. Lett.*, 2022, **4**, 1053–1057.
- 63 P. Wang, X. Li, P. Zhang, X. Zhang, Y. Shen, B. Zheng, J. Wu, S. Li, Y. Fu, W. Zhang and F. Huo, Transitional MOFs: Exposing metal sites with porosity for enhancing catalytic reaction performance, *ACS Appl. Mater. Interfaces*, 2020, **12**, 23968–23975.
- 64 X. Hou, J. Wang, B. Mousavi, N. Klomkliang and S. Chaemchuen, Strategies for induced defects in metal-





- organic frameworks for enhancing adsorption and catalytic performance, *Dalton Trans.*, 2022, **51**, 8133–8159.
- 65 J. Ren, M. Ledwaba, N. M. Musyoka, H. W. Langmi, M. Mathe, S. Liao and W. Pang, Structural defects in metal-organic frameworks (MOFs): Formation, detection and control towards practices of interests, *Coord. Chem. Rev.*, 2017, **349**, 169–197.
  - 66 S. Dissegna, K. Epp, W. R. Heinz, G. Kieslich and R. A. Fischer, Defective metal-organic frameworks, *Adv. Mater.*, 2018, **30**, 1704501.
  - 67 S. M. Shaikh, P. M. Usov, J. Zhu, M. Cai, J. Alatis and A. J. Morris, Synthesis and defect characterization of phase-pure Zr-MOFs based on meso-tetracarboxyphenylporphyrin, *Inorg. Chem.*, 2019, **58**, 5145–5153.
  - 68 W. Meng, H. Wu, X. Bi, Z. Huo, J. Wu, Y. Jiao, J. Xu, M. Wang and H. Qu, Synthesis of ZIF-8 with encapsulated hexachlorocyclotriphosphazene and its quenching mechanism for flame-retardant epoxy resin, *Microporous Mesoporous Mater.*, 2021, **314**, 110885.
  - 69 B. Hou, X. Song, K. Song, Z. Geng, Y.-T. Pan, P. Song and R. Yang, Synchronous preparation and modification of LDH hollow polyhedra by polydopamine: Synthesis and application, *J. Colloid Interface Sci.*, 2024, **654**, 235–245.
  - 70 H. Zhao, B. Yuan, Y. Zhan, F. Yang, J. Zhou, C. Qi, C. Lei and Y. Li, Upgrading the pore-size scale of MIL-53 from microporous to macroporous for adsorbing triethyl phosphate and reducing the fire risk of polystyrene, *Composites, Part A*, 2022, **159**, 107003.
  - 71 G. Zhang, Y. Dong, M. Yao, Y. Cui, W. Meng, S. Wang, H. Qu and J. Xu, Preparation of a MOF flame retardant containing phosphazene ring and its effect on the flame retardant of epoxy resin, *React. Funct. Polym.*, 2023, **191**, 105670.
  - 72 L. Liu, M. Yao, H. Zhang, Y. Zhang, J. Feng, Z. Fang and P. Song, Aqueous self-assembly of bio-based flame retardants for fire-retardant, smoke-suppressive, and toughened polylactic acid, *ACS Sustainable Chem. Eng.*, 2022, **10**, 16313–16323.
  - 73 S. Qiu, W. Yang, X. Wang and Y. Hu, Phthalocyanine zirconium diazo passivation of black phosphorus for efficient smoke suppression, flame retardant and mechanical enhancement, *Chem. Eng. J.*, 2023, **453**, 139759.
  - 74 Y. Zhou, L. Wang, L. Ding, W. Yang, C. Zhang, D. Liu, W. Hu and Y. Hu, Innovative design and preparation of hierarchical BP-OH@HAP structure: Study on flame retardancy and mechanical characteristics of upr nanocomposites, *ACS Mater. Lett.*, 2023, **2870–2876**, DOI: [10.1021/acsmaterialslett.3c00865](https://doi.org/10.1021/acsmaterialslett.3c00865).
  - 75 Z. Sun, Y. Liao, S. Zhao, X. Zhang, Q. Liu and X. Shi, Research progress in metal-organic frameworks (MOFs) in CO<sub>2</sub> capture from post-combustion coal-fired flue gas: Characteristics, preparation, modification and applications, *J. Mater. Chem. A*, 2022, **10**, 5174–5211.
  - 76 K. Gong, L. Cai, C. Shi, F. Gao, L. Yin, X. Qian and K. Zhou, Organic-inorganic hybrid engineering MXene derivatives for fire resistant epoxy resins with superior smoke suppression, *Composites, Part A*, 2022, **161**, 107109.
  - 77 J. Huang, W. Guo, X. Wang, H. Niu, L. Song and Y. Hu, Combination of cardanol-derived flame retardant with SiO<sub>2</sub>@MOF particles for simultaneously enhancing the toughness, anti-flammability and smoke suppression of epoxy thermosets, *Compos. Commun.*, 2021, **27**, 100904.
  - 78 C.-C. Hou, Y. Wang, L. Zou, M. Wang, H. Liu, Z. Liu, H.-F. Wang, C. Li and Q. Xu, A gas-steamed mof route to P-doped open carbon cages with enhanced zn-ion energy storage capability and ultrastability, *Adv. Mater.*, 2021, **33**, 2101698.
  - 79 J. Yang, K. Li and J. Gu, Hierarchically macro-microporous Ce-based mofs for the cleavage of DNA, *ACS Mater. Lett.*, 2022, **4**, 385–391.
  - 80 K. Li, J. Yang and J. Gu, Hierarchically porous MOFs synthesized by soft-template strategies, *Acc. Chem. Res.*, 2022, **55**, 2235–2247.
  - 81 T. Qiu, S. Gao, Z. Liang, D.-G. Wang, H. Tabassum, R. Zhong and R. Zou, Pristine hollow metal-organic frameworks: Design, synthesis and application, *Angew. Chem.*, 2021, **60**, 17314–17336.
  - 82 Z. Tian, Q. Sui, C. Zhang, C. Xiang, L. Sun, F. Xu and Y. Zou, Nanoarchitectonics of metal-organic frameworks on nickel-cobalt hydroxides hollow prisms for supercapacitors, *J. Energy Storage*, 2023, **72**, 108052.
  - 83 V. Unnikrishnan, O. Zabihi, Q. Li, M. Ahmadi, R. Yadav, E. N. Kalali, K. Tanwar, A. Kiziltas, P. Blanchard, D.-Y. Wang and M. Naebe, Organophosphorus-functionalized zirconium-based metal-organic framework nanostructures for improved mechanical and flame retardant polymer nanocomposites, *ACS Appl. Nano Mater.*, 2021, **4**, 13027–13040.
  - 84 J. Zhang, Z. Li, L. Zhang, Y. Yang and D.-Y. Wang, Green synthesis of biomass phytic acid-functionalized UiO-66-NH<sub>2</sub> hierarchical hybrids toward fire safety of epoxy resin, *ACS Sustainable Chem. Eng.*, 2019, **8**, 994–1003.

